Chemosphere 253 (2020) 126739

Contents lists available at ScienceDirect

Chemosphere

journal homepage: www.elsevier.com/locate/chemosphere

Heterologous expression and functional study of nitric oxide reductase catalytic reduction peptide from *Achromobacter denitrificans* strain TB

Cong Chen [a], Yu Wang [a], Huan Liu [a], Yi Chen [a], Jiachao Yao [b], Jun Chen [b, *], Dzmitry Hrynsphanb [c], Savitskaya Tatsianab [c]

[a] College of Environmental, Zhejiang University of Technology, Hangzhou, 310032, PR China
[b] College of Biological and Environmental Engineering, Zhejiang Shuren University, Hangzhou, 310021, PR China
[c] Research Institute of Physical and Chemical Problems, Belarusian State University, Minsk, 220030, Belarus

HIGHLIGHTS

- NOR was successfully cloned and expressed under the optimal induction conditions.
- The relative expression abundance of the *norB* gene was increased by 16.6 times.
- Recombinant *E. coli* can reduce NO to N_2O and express active NorB proteins.
- The core peptide of TB NOR catalytic structure can independently degrade NO.

ARTICLE INFO

Article history:
Received 18 October 2019
Received in revised form
21 January 2020
Accepted 4 April 2020
Available online 12 April 2020

Handling Editor: Can Wang

Keywords:
Nitric oxide reductase peptide
Achromobacter denitrificans
Heterologous expression
Reducing property

ABSTRACT

Biological denitrification is a promising and green technology for air pollution control. To investigate the nitric oxide reductase (NOR) that dominates NO reduction efficiency in biological purification, the heterologous prokaryotic expression system of the *norB* gene, which encodes the core peptide of the catalytic reduction structure in the NOR from *Achromobacter denitrificans* strain TB, was constructed in *Escherichia coli* BL21 (DE3). Results showed that the 1218 bp-long *norB* gene was expressed at the highest level under 1.0 mM IPTG for 5 h at 30 °C, and the relative expression abundance of *norB* in recombinant *E. coli* was increased by 16.6 times compared with that of the wild-type TB. However, the NO reduction efficiency and NOR activity of strain TB was 2.7 and 1.83 times higher than those of recombinant *E. coli*, respectively. On the basis of genomic reassembly and protein structure modeling, the core peptide of the NOR catalytic reduction structure from *Achromobacter* sp. TB can independently exert NO reduction. The low NO degradation efficiency of recombinant *E. coli* may be due to the lack of a NorC-like structure that increases the enzyme activity of the NorB protein. The results of this study can be used as basis for further research on the structure and function of NOR.

1. Introduction

Nitric oxide (NO) is a major atmospheric pollutant that causes many environmental problems, such as acid rain, acid fumes, photochemical smog, and ozone depletion (Abalos et al., 2012; Hong et al., 2017). Recently, bioprocesses have received considerable interest because they offer several advantages over conventional technologies for the flue gas cleaning (Kennes et al., 2009). The main principle of these methods in removing NO is microbial-dominated denitrification; that is, the nitric oxide reductase (NOR) in the microorganism can bind and reduce NO to non-toxic and harmless N_2 by continuous enzymatic reactions. Therefore, in-depth studies on the characteristics of NOR are crucial for improving the NO removal efficiency of biological purification.

NOR exists in most denitrifying bacteria, and some pathogenic bacteria that cannot perform denitrification but contain NOR for their own detoxification (Zumft, 2005; Tomasek et al., 2017). NOR is

* Corresponding author.
E-mail address: bec@zjut.edu.cn (J. Chen).

https://doi.org/10.1016/j.chemosphere.2020.126739
0045-6535/

a metalloenzyme containing a non-heme Fe center that reduces NO to N_2O, using two protons and two electrons. On the basis of the characteristics of electron donor and enzyme composition in the reduction process, NOR can be divided into the following three categories (Wasser et al., 2002; Ramos et al., 2017): cNOR with non-heme Fe, qNOR with non-heme Fe, and qCuANOR with Fe and Cu. cNOR is composed of NorB and NorC subunits. According to the cNOR crystal structure from *Pseudomonas aeruginosa* (Hino et al., 2010), the NorB subunit has 12 transmembrane helixes and contains low-spin heme b and high-spin heme b_3. Heme b_3 contains a non-heme Fe—FeB in addition to heme Fe. Heme Fe and FeB are linked by μ-oxygen bridge or carboxylate bridge to form the Fe—FeB catalytic reduction activity center. NorC subunit is an anchor membrane protein containing a low-spin heme c located in the periplasmic region (Gomes et al., 2019). The first separation of qNOR is purified by the His-tagged protein in the denitrifying bacteria *Ralstonia eutropha* (Matsumoto et al., 2012; Tosha and Shiro, 2013). qNOR is an 84 kDa single subunit protein encoded by a single gene, *norB* or *norZ*. It is commonly found in pathogenic bacteria. When the electron donor is hydroquinone, the qNOR protein exhibits NO reduction activity. Compared with cNOR, qNOR lacks heme c, but contains high-spin heme b_3, low-spin heme b, and FeB. In the transmembrane region, qNOR contains 14 transmembrane helices; outside the cell, qNOR has an alpha-helical hydrophilic domain (Nadeau et al., 2019). The N-terminus of qNOR contains a peptide chain of 280 amino acid residues that can be folded into two alpha transmembrane helices. This domain sequence is very similar to the NorC protein sequence in cNOR.

Butland et al. (2001) found that *Escherichia coli* could not express the NorCB complex of *Paracoccus denitrificans* when the auxiliary gene *norQDEF* was deleted. However, Kahle et al. (2018) showed that *E. coli* can still produce stable NorCB complexes in the absence of auxiliary genes. These results indicate that the encoding genes of NOR from different denitrifying bacteria are different, and whether the *norB* gene can be correctly expressed in *E. coli* cannot be determined due to the difference in the source bacteria. Cramm et al. (1999) found that the NOR in the denitrifying bacteria *R. eutropha* is only encoded by a single gene, *norB*. Sakurai et al. (2017) found that *norC* can encode NorC protein alone, and monoclonal *norB* gene cannot be expressed in *E. coli*. However, they did not investigate the activity of enzymes or the performance of recombinant bacteria, and functional studies based on proteins structure encoded by a single *norB* gene are limited.

To date, only three *Achromobacter denitrificans* have been completely sequenced according to the National Center for Biotechnology Information database. Sequencing and quantitative amplification by real-time PCR of the denitrification genes showed that removal pathway of strain YG-24 and *Pseudomonas stutzeri* strain XL-2 (Li et al., 2015; Zhao et al., 2018). Yoon et al. (2016) demonstrated that *Dechloromonas denitrificans* possessed a clade II nosZ gene. However, the complete denitrifying genes in individual bacteria have not been systematically analyzed. In previous studies, we have successfully achieved the heterologous expression of *nosZ* gene in *E. coli* (Wang et al., 2018). In the present study, the genome sequence of denitrifying bacteria *A. denitrificans* strain TB was obtained by de novo genome sequencing method. The gene map and sequence information related to denitrification were identified. Subsequently, the core gene *norB* of the catalytic reduction structure in the NOR from *Achromobacter* sp. TB was cloned, and the prokaryotic expression vector of the *norB* gene was constructed to obtain recombinant *E. coli* BL21 (DE3)-pET28a-*norB*. Moreover, the NO degradation capability of recombinant *E. coli* and strain TB was evaluated.

2. Materials and methods

2.1. Plasmids and enzymes

Achromobacter sp. TB (GenBank accession no. JQ044686), was isolated from a rotating drum biofilter for NO removal (Chen et al., 2016). *E. coli* DH5α, *E. coli* BL21 (DE3), and plasmids pGEM-T and pET28a were purchased from TaKaRa Biotechnology Co., Ltd. T4 DNA ligase, *EcoR* I, and *Xho* I were purchased from Thermo Fisher Scientific., Inc. PCR reagents were bought from Vazyme Biotech Co., Ltd. SYBR® qPCR Mix was obtained from Toyobo Co., Ltd.

2.2. De novo genome sequencing of Achromobacter sp. TB

Genomic DNA was extracted from strain TB. The extracted DNA was sent to GENEWIZ Biotechnology Co., Ltd. for sequencing. The appropriate amount of DNA was randomly broken into fragments of approximately 10 kb. The HiSeq library and SMRTbell library were constructed according to the manufacturer's instructions. Subsequent second- and third-generation sequencing was performed on the Illumina and PacBio Sequel sequencing platforms, respectively.

The pass filter data were processed to clean the data, which were then assembled into second- and third-generation genome assemblies. The second-generation genome assembly data were compared with the third-generation assembly data, and the difference was corrected on the basis of the second-generation sequencing result, resulting in the final corrected genomic sequence of *Achromobacter* sp. TB.

The open reading frame (ORF) from the genomic sequence of strain TB was predicted using the Prodigal software (version 2.6.3). According to the annotation results of the database (KEGG, GO, COG, Nr), the composition, structure, and position information of the denitrifying gene cluster in *Achromobacter* sp. TB were analyzed.

2.3. Gene cloning and bioinformatics analysis of norB gene

The genomic DNA of *Achromobacter* sp. TB was used as DNA template for PCR. PCR was performed in a Mastercycler gradient (Bio-Rad, USA) using the following primers designed according to the *norB* gene reference sequence, which is derived from the genomic sequence of *Achromobacter* sp. TB: *norB*-F (5′- GAATTCATGAGCGCGGTCGGCAATACGCCCAGCGCCGAGA -3′) and *norB*-R (5′- CTCGAGGGCCCTGGATGTAGTACAGCGAGAGGGCGGGTTG -3′). PCR mixture (50 μL) consisted of 25 μL 2 × Phanta Max Buffer, 1 μL dNTP Mix (10 mM), 2 μL oligonucleotide primers, 1 μL Phanta polymerase, 2 μL template DNA, and 17 μL deionized water. The mixture was pre-denatured at 95 °C for 3 min, followed by 33 cycles of denaturation at 95 °C for 0.5 min; annealed at 55 °C for 0.5 min; extended at 72 °C for 1.5 min; and subjected to a final extension at 72 °C for 5 min. The PCR product obtained using QIAquick Gel Extraction Kit was subjected to an "A tail" treatment using TIANGEN 2 × Taq PCR Master Mix kit (TIANGEN). It was then ligated into pGEM-T plasmid to form a TA clone and sequenced.

The *norB* sequences were aligned by BLAST, and a phylogenetic tree was constructed using the neighbor-joining method with 1000 bootstrap trials by MEGA software (version 7.0.26). The basic secondary structure and the helical transmembrane region of the NorB protein were analyzed using an online website (https://www.predictprotein.org/). Using another online website (https://swissmodel.expasy.org/), the protein three-dimensional structure was modeled on the basis of the amino acid sequence and structure of qNOR from *Neisseria meningitidis* (PDB ID: 6fwf.1. A), and it was edited using Discovery Studio Visualizer 4.5 software.

2.4. Construction of recombinant E. coli BL21 (DE3)-pET28a-norB

For the construction of recombinant *E. coli*, the pGEM-T-*norB* and pET28a plasmids were simultaneously digested with *EcoR* I and *Xho* I, and the released *norB* gene was subsequently ligated into the treated pET28a plasmid to construct the gene expression vector pET28a-*norB*. The expression vector pET28a-*norB* was then transformed into *E. coli* BL21 (DE3) to obtain recombinant *E. coli* BL21 (DE3)-pET28a-*norB* for expression. Conditions affecting *norB* gene expression, such as inducer final concentration (0.2, 0.5, 1.0, 1.5, 2.0, and 2.5 mM), induction time (2, 3, 4, 5, 6, and 7 h), and induction temperature (22 °C, 25 °C, 28 °C, 30 °C, 33 °C, and 37 °C) were optimized. SDS-PAGE was used to detect the expression level.

2.5. Real-time fluorescence quantitative PCR (RT-qPCR) analysis of norB gene

The recombinant *E. coli* was cultured at 37 °C and 160 rpm until the middle of the logarithmic growth phase, and a final concentration of 1.0 mM IPTG inducer was added for induction at 30 °C and 160 rpm for 5 h. Strain TB and *E. coli* containing the empty plasmid pET28a were used as positive and negative controls, respectively. The total RNA of the three bacterial liquids was extracted, and the RNA was reverse-transcribed into cDNA using the AMV First Strand cDNA Synthesis Kit (Sangon). The gene quantitation was detected by relative quantitative PCR method as described before (Mazza and Mazzette, 2014). The relative abundance of functional genes was calculated by the ratio of the functional gene abundance to the 16S rRNA gene abundance.

2.6. Comparison of NO reduction performance and enzyme activity

The recombinant *E. coli* was cultured and induced as described above. Strain TB was cultured at 30 °C for the same time. The bacterial cell pellet was collected and washed and then transferred to 50 mL inorganic salt medium (pH 7.0) containing (per liter) 1.7 g/L $NaHCO_3$, 0.942 g/L $K_2HPO_4 \cdot 3H_2O$, 0.234 g/L KH_2PO_4, 0.98 g/L NaCl, 0.2 g/L $MgCl_2$, 0.011 g/L $CaCl_2$, 0.016 g/L $FeCl_3$, and 5 mL trace element solution. The trace element solution comprised the following (per liter): 0.088 g/L $ZnCl_2$, 0.06 g/L $MnCl_2 \cdot 4H_2O$, 0.01 g/L KI, 0.1 g/L $Na_2MoO_4 \cdot 2H_2O$, and 0.05 g/L H_3BO_3. After rinsing with argon for 20 min, the internal space of the shake flask was guaranteed to be completely oxygen deficient. Approximately 1 mL NO pure gas was injected into the sealed oxygen-free shake flask using an Agilent gas-tight syringe, and the initial concentration of NO and N_2O in the shake flask and the remaining concentration after 13 h of degradation were measured using a gas chromatograph.

The proteins from strain TB and recombinant *E. coli* after induction culture was extracted using Minute™ total protein extraction kit (Invent). The extracted proteins were assayed for NOR activity in accordance with the method of Chen et al. (2019). In brief, 100 μL extracted proteins was injected into an anaerobic reaction chamber with 2 mL compound comprising 10 mM PBS buffer (pH 7.4), 5 mM sodium dithionite, 10 mM electron donor, and 1 mM electron acceptor. Methyl viologen was used as the electron donor, whereas NO was used as the electron acceptor for NOR. After incubating for 30 min at 25 °C, the consumptions of NO were measured to calculate the specific activity of NOR.

2.7. Analytical methods

The reduction of NO was determined using Molecular Sieve 5A Packed Column (3 m × 4 mm) at 100 °C on a gas chromatograph with a thermal conductivity detector (Fuli 9790II). The injector and detector temperatures were both 120 °C, and the carrier gas was Ar at a pressure of 0.4 MPa. The formation of N_2O was measured using HP-5 capillary column (30 m × 320 μm × 0.25 μm) at 40 °C on a gas chromatograph with an electron capture detector (Agilent 6890 N). The injector and detector temperatures were 100 °C and 300 °C, respectively, and the carrier gas was N_2 with a flow rate of 2 mL/min. T-test at a 5% probability level was performed and was reported as p-values. All experiments were performed in triplicate, and data were presented as means ± standard deviation.

3. Results

3.1. De novo sequencing of Achromobacter sp. TB

3.1.1. Genomic sequence of strain TB

The genomic sequencing results showed that *Achromobacter* sp. TB contained only one circular genome sequence and no other plasmid sequences. The total genome length was 6,692,590 bp, the genome coverage was 100.00%, and the content of bases G and C (GC) was 67.39%. The Prodigal software predicted that the genome contains 6230 ORFs with an average length of 963.79 bp and a total length of 6,004,407 bp, covering 89.72% of the genome sequence. Through the sequence alignment with the Rfam database, 158 total non-coding RNA (ncRNA) were found in the genome, of which 41 were rRNAs and 62 were tRNAs, and 55 other ncRNAs such as snRNA, snoRNA, and microRNA were involved. Repeated sequence analysis showed that the genome contained no short repeat sequence of less than 100 bp, no DNA transposons, and no satellite RNA. The genome contained 127 long repeat regions with a repeat length of 100 bp or more, of which 1200 bp or more were repeat sequences, accounting for 54.33% (Fig. 1).

3.1.2. Identification of denitrifying genes in strain TB

Four reductases were involved in the bacterial denitrification, namely, nitrate reductase (NaR), nitrite reductase (NiR), NOR, and nitrous oxide reductase (N_2OR).

In strain TB, both *nar* and *nap* were presented in the form of gene clusters. The *nar* gene cluster was located on the antisense strand of the genome with a total length of 15.1 kb. It contained eight ORFs, namely, *nark_1*, *nark_2*, *narG*, *narH*, *narJ*, *narI*, *narQ,* and *narL*. Among them, the longest gene was *narG* with a length of 3741 bp, encoding the α subunit of NaR; *narH* and *narI* encoded the β and γ subunits of NaR, respectively; and *narJ* was responsible for the assembly of NaR. These eight genes were transcribed in the same direction on the chromosome (Fig. 2A). The genes were arranged regularly, and no gap was present before and after the coding region. Only four bases overlapped between *narH* and *narG*. The *nap* gene cluster was located on the genomic sense strand with a total length of 4133 bp, containing five ORFs, namely, *napE*, *napD*, *napA*, *napB*, and *napC* (Fig. 2A). *napA* was the longest gene (2496 bp), encoding the large subunit of the periplasmic NaR, and *napB* encoded a small subunit of this enzyme. The NapC protein, which was a transmembrane component that interfaced with the NapB protein, acted as an electron transporter. The *nap* gene cluster was continuously arranged on the chromosome and contained no other genes inside.

The Nir of strain TB was encoded by the *nirK* gene. In addition to conventional Nir, an NADH-dependent NiR encoded by the *nirBDC* gene was also present in the strain TB (Fig. 2B). The NADH-dependent Nir was expressed under anaerobic conditions, which contained a soluble siroheme and a [4Fe−4S] cluster. It can reduce nitrite to ammonia, and NO is only used as an intermediate in the reduction process (Wang and Gunsalus, 2000; Sofya et al., 2005; Nasr and Akbari Eidgahi, 2014).

The NOR of strain TB was encoded by the *norB* gene with a length of 1215 bp and regulated by the *norR* gene with a length of

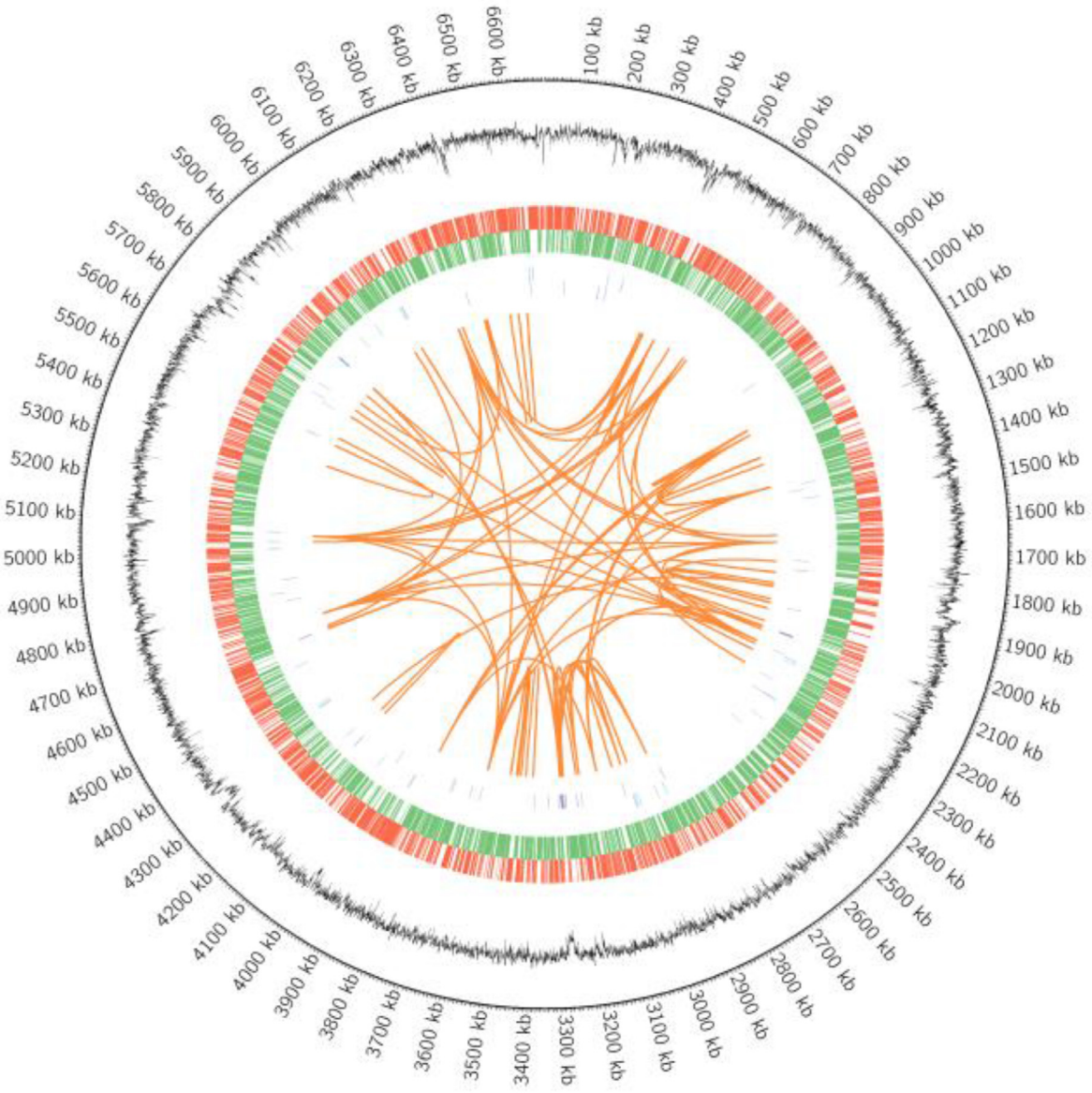

Fig. 1. Genome circle of strain TB. From the outside to the inside. The first circle is the genomic location information, the second circle is the GC content information. The third circle is the coding gene on the positive chain (marked in red), and the fourth circle is the coding gene on the negative chain (marked in green). The fifth circle is the ncRNA information on the positive chain (marked in blue). The sixth circle is the ncRNA information on the negative chain (marked in purple), and the seventh circle is the long fragment repeat information in the genome (marked in orange). (For interpretation of the references to colour in this figure legend, the reader is referred to the Web version of this article.)

1530 bp. The *norC* gene was not included in the genome. The 1.9 kb downstream of the *norB* gene was the location of *nirK* coding the cupric Nir. The 1.9 kb between *norB* and *nirK* contained two ORFs, the protein encoded by the upstream ORF may be the NorD protein, and the downstream ORF encoded Fnr family transcriptional regulator (Fig. 2C).

The coding gene for N_2OR in strain TB was clustered to form a *nos* gene cluster with a total length of 7807 bp. It included six ORFs, namely, *nosR*, *nosZ*, *nosD*, *nosF*, *nosY*, and *nosL*. The *nosR* gene with length of 2247 bp encoded the transcriptional regulator, and the structural gene *nosZ* with a length of 1917 bp encoded the N_2OR protein. The length of *nosDFYL* was decreased in turn. *nosDFYL* encoded the N_2OR accessory protein, Cu-processing system ATP-binding protein, Cu-processing system permease protein, and copper chaperone. The *nos* gene cluster was located on the antisense strand of the genome and was transcribed in the same direction. The intergenic arrangement was relatively compact and contained no other genes (Fig. 2D).

3.2. Gene cloning and NOR expression in E. coli BL21 (DE3)

3.2.1. TA cloning

The *norB* gene encoding NOR in *Achromobacter* sp. TB was obtained by TA cloning and sequencing. It had a total length of 1218 bp and encoded a protein of 405 amino acids with a theoretical molecular mass of 44.7 kDa. The results of BLAST homologous alignment revealed that the similarity between the *norB* sequence from strain TB and the nucleotide sequence encoding the large subunit NorB protein of NOR from *A. denitrificans* strain PR1 was as high as 99%. The phylogenetic tree showed that the confidence of homology with *norB* gene from *Achromobacter* sp. TB and *Achromobacter* sp. PR1 was 100 (Fig. 3).

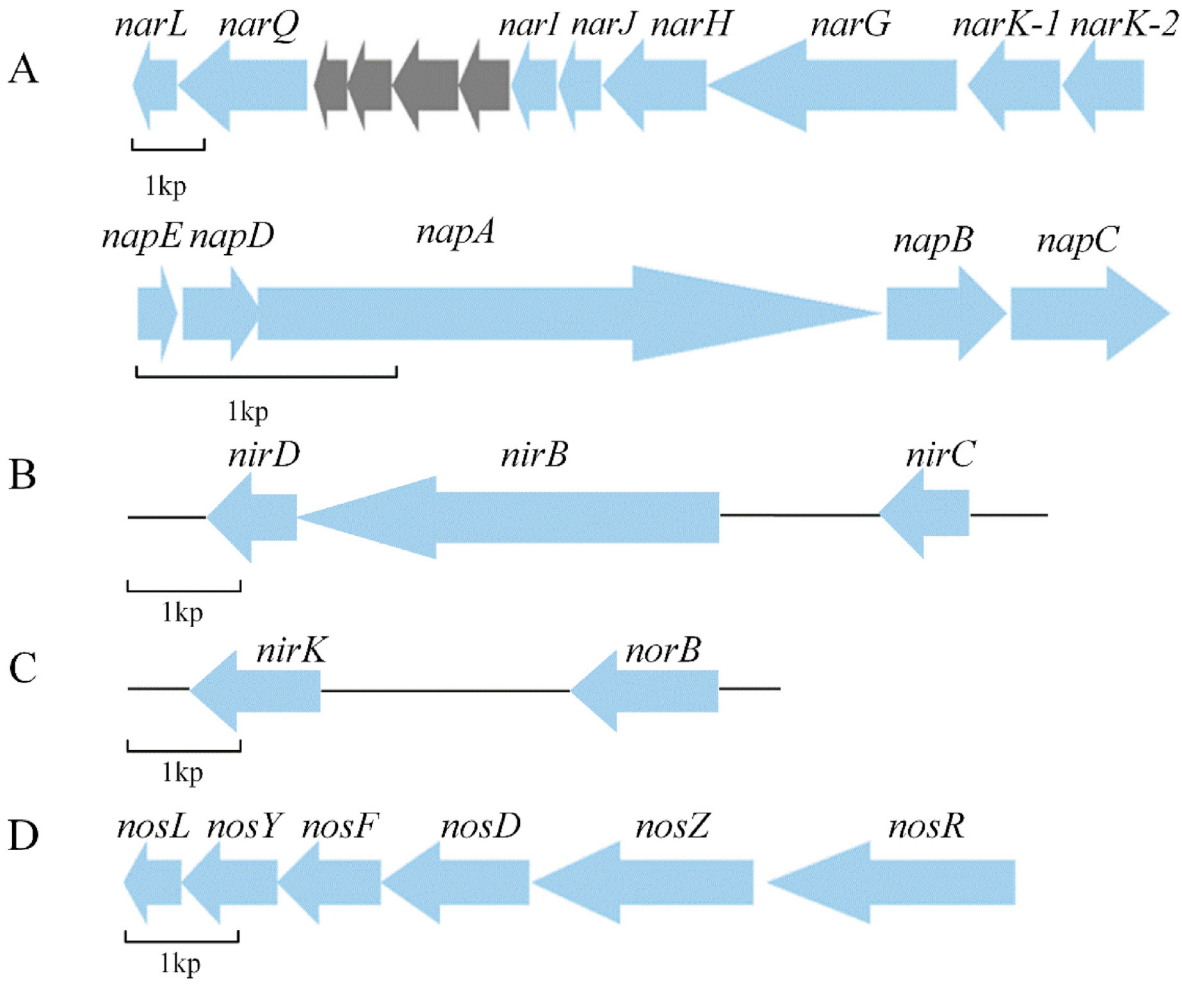

Fig. 2. Schematic diagram of denitrifying genes in strain TB. (A) *nar* and *nap* gene cluster; (B) *nir* gene cluster; (C) *nor* gene cluster; (D) *nos* gene cluster. The direction of the arrow indicates the direction of transcription. The blue arrow represents the denitrification gene and the gray arrow represents other genes. Arrow shows the direction of transcription and blue arrow represents the denitrification gene. (For interpretation of the references to colour in this figure legend, the reader is referred to the Web version of this article.)

3.2.2. Optimized expression of NOR in E. coli BL21 (DE3)

The expression vector pET28a-*norB* was transferred to the recipient cell to obtain a recombinant engineered strain *E. coli* BL21 (DE3)-pET28a-*norB*. IPTG was used to induce *norB* gene expression. *E. coli* containing empty vector pET28a (negative control) showed a band at 45 kDa, indicating that *E. coli* BL21 (DE3) can produce a 45 kDa endogenous protein (Fig. 4A). Recombinant *E. coli* without IPTG induction also showed a band at 45 kDa, and the brightness of the band was similar to that of the negative control, indicating that the band was likely derived from endogenous expression of *E. coli*. The target band appeared at 45 kDa after IPTG induction of recombinant *E. coli*. The size was consistent with the predicted molecular mass of NorB protein. The band brightness was slightly brighter than that of the negative control, suggesting that the NorB protein may be expressed under the induction of IPTG. Strain TB showed no significant bands at 45 kDa, indicating that the size of the NOR protein in strain TB may not be 45 kDa.

The pre-induction inoculum OD_{600} was set at 0.6. At this time, the recombinant *E. coli* was in the pre-metaphase stage of the logarithmic phase (Fig. S1), which was the most favorable condition for gene expression (Noi and Chung, 2017). Different IPTG concentrations were selected to investigate the expression of the *norB* gene. As a result, the expression level of the NorB protein varied with the concentration of IPTG. At 1.0 mM IPTG, the expression level of the NorB protein reached the highest levels (Fig. 4B).

The target band at 45 kDa did not change substantially within 2–4 h of induction (Fig. 4C) but became brighter at 5 h. After induction for 6–7 h, the amount of target protein was considerably higher than that after induction for 2–4 h. However, it was relatively lower than that induced for 5 h. The general trend is that the yield of the protein increases with increasing induction time. Given that high temperature is not conducive to gene expression, low temperature will delay the growth of bacteria. The optimal induction time for *norB* gene expression was 5 h.

The results of the induced temperature investigation showed that the target protein bands were all bright at different temperatures, showing almost no difference (Fig. 4D). Considering the actual growth environment of *E. coli* and the conditions provided by the laboratory, the optimal induction temperature was set to 30 °C.

3.2.3. RT-qPCR of norB gene

RT-qPCR analysis was performed to quantify the expression abundance of *norB* in recombinant *E. coli* and strain TB. As shown in Fig. 5, RT-qPCR results showed that the relative expression abundance of *norB* in recombinant *E. coli* without IPTG induction was 0.28% (the recombinant *E. coli* 16S rRNA was used as internal reference gene), indicating that there was a phenomenon of background expression in recombinant *E. coli*. The relative expression

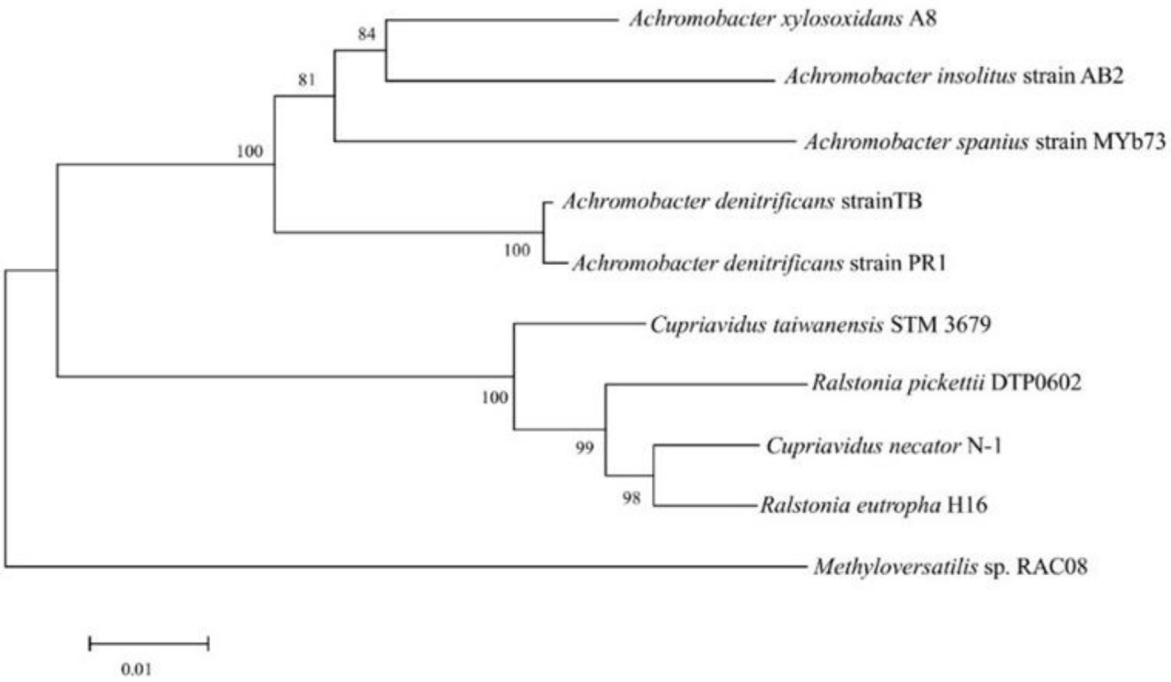

Fig. 3. Phylogenetic tree of *norB* gene in *Achromobacter* sp. TB.

abundance of *norB* in recombinant *E. coli* induced by IPTG increased significantly ($p < 0.05$), reaching 0.83%, which was 2.96 times higher than that of uninduced recombinant *E. coli*. This finding indicated that IPTG promoted the transcription of *norB* substantially. Recombinant *E. coli* BL21 (DE3)-pET28a-*norB* was successfully induced and expressed. The relative expression abundance of *norB* in strain TB was only 0.05% (the strain TB 16S rRNA was used as internal reference gene), which was consistent with the above SDS-PAGE electrophoresis results (Fig. 4A). Therefore, *norB* in strain TB was probably not expressed or not transcribed alone. It may have combined with some other sequence fragments to transcribe and express a NOR protein with a molecular mass of more than 45 kDa. The RT-qPCR results in *E. coli* harboring empty vector pET28a were negative (data not shown).

3.3. Bacterial reduction performance comparison

The gas chromatographic results of N_2O in the NO reduction system from the recombinant *E. coli* are shown in Fig. S2. The N_2O target peak was not observed at approximately 2.92 min, but it appeared after degrading for 13 h. According to the N_2O peak area—N_2O concentration standard curve, the concentration of N_2O produced in the NO reduction system of recombinant *E. coli* was 96.27 ppm after 13 h. The results showed that the recombinant *E. coli* could degrade 12.39% of NO within 13 h (Fig. 6A). Obviously, the NO reduction efficiency of strain TB (33.48%) was strengthened 2.7 times compared with that of recombinant *E. coli*, and the NO reduction system produced 200.16 ppm of N_2O in 13 h.

The total enzyme activity of strain TB was 0.56 μmol-NO/min/mg protein (Fig. 6B), which was 1.83 times higher than that of recombinant *E. coli*. In addition, almost no NOR activity was observed in the negative control group. These results indicated that recombinant *E. coli* can indeed reduce NO to N_2O, and the *norB* gene was not only successfully expressed in recombinant *E. coli* but also correctly translated into an active NorB protein.

4. Discussion

The A. *denitrificans* strain TB showed better NO reduction efficiency in the biological drum reactor. Therefore, we attempted to explore the structure and function of the enzyme that exerts high reduction efficiency and find a solution from a molecular perspective to further improve the NO reduction efficiency of the enzyme. Unlike other *Achromobacter* species (Vedler et al., 2004; Vincenzo et al., 2014), *Achromobacter* sp. TB does not contain plasmids. Forty-two coding genes responsible for denitrification were all located on the unique genome sequence. Some of these genes were scattered over the genome, and the other part constituted the *nar*, *nap*, and *nos* denitrifying gene clusters. The *nir* and *nor* genes were not clustered. The *nap*, *nir*, and *nor* genes were relatively close on the chromosome, forming the *nap-nir-nor* "island," and *nar* and *nos* were distributed at both ends of the *nap-nir-nor* "island" (Fig. S3). Moreover, the distance between the *nos* gene cluster and the *nap-nir-nor* "island" was 4432 kb, which explained why N_2O was easily accumulated as an intermediate in the bacterial denitrification (Wang et al., 2018).

The conventional denitrifier *Pseudomonas stutzeri* A1501 (Yan et al., 2008) and *A. xylosoxidans* NCTC10807 (Accession: NZ LN831029) were selected, and their denitrification genes were compared. *P. stutzeri* A1501 contained only the *nar* gene cluster without the *nap* gene cluster. Moreover, the *nar*, *nir*, and *nor* gene clusters in *P. stutzeri* A1501 had different gene compositions and transcription directions compared with those in strain TB (Fig. S4). However, the gene composition of the *nar*, *nap*, *nir*, *nor*, and *nos* gene clusters in *A. xylosoxidans* NCTC10807 was exactly the same as in the strain TB, differing only in the gene transcription direction (Fig. S4). The gene for the *Achromobacter* NOR was identified by BLAST analysis. Surprisingly, we found only a *norB* homolog, whereas most denitrifiers possessed a two-subunit enzyme encoded by *norC* and *norB*. In addition, the *norB* gene in *A. xylosoxidans* NCTC10807 was 2286 bp long, nearly twice as long as *norB* in strain TB (1218 bp). It is the largest difference in their denitrification

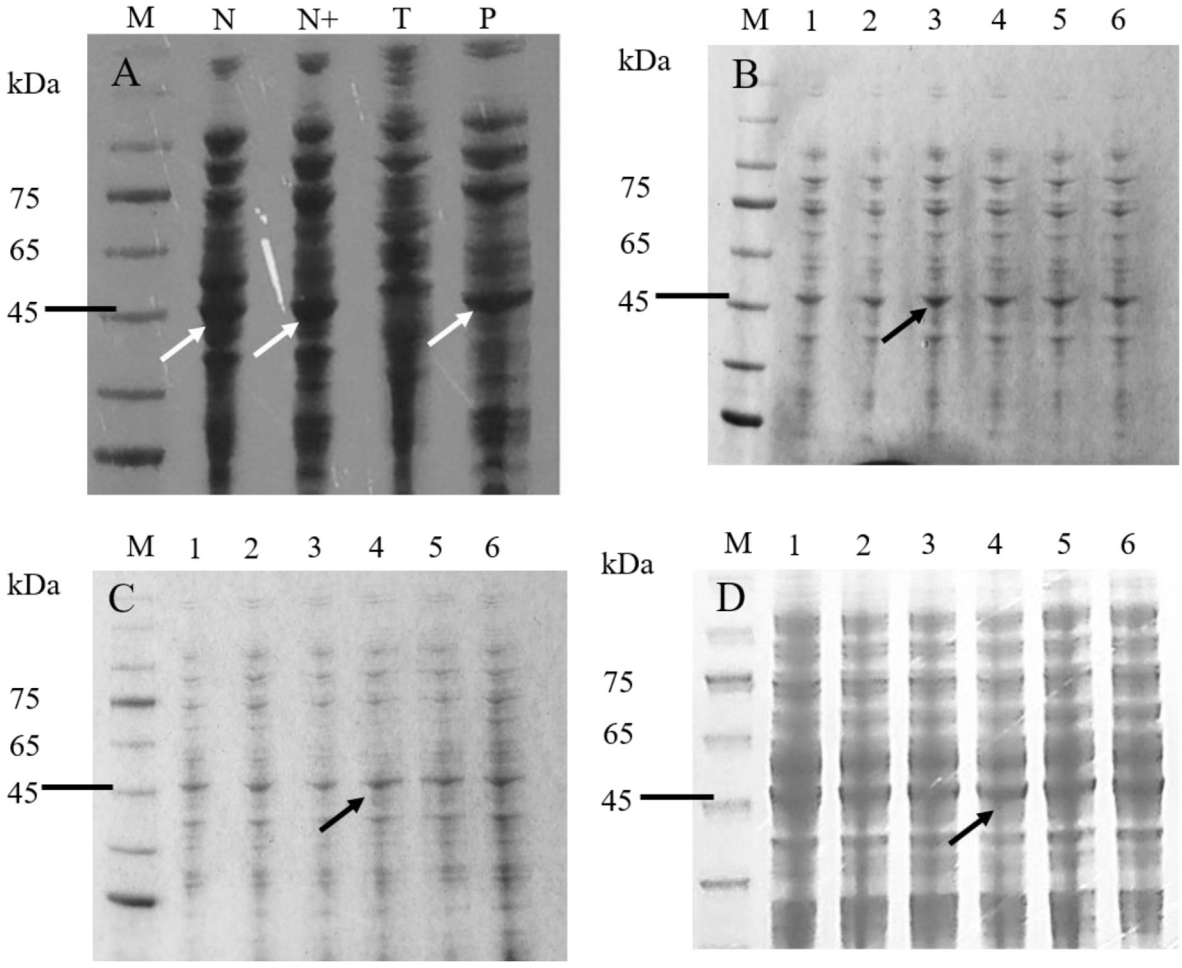

Fig. 4. SDS-PAGE electrophoresis analysis of NorB protein. (A) M: Protein marker; N: Total protein of recombinant *E. coli* without IPTG induction; N+: Total protein of recombinant *E. coli* with IPTG induction; T: Total protein of wild strain TB; P: Total protein of *E. coli* containing empty vector pET28a. (B) IPTG concentration, 1: 0.2 mM; 2: 0.5 mM; 3: 1.0 mM; 4: 1.5 mM; 5: 2.0 mM; 6: 2.5 mM. (C) Induction time, 1: 2 h; 2: 3 h; 3: 4 h; 4: 5 h; 5: 6 h; 6: 7 h. (D) induction temperature, 1: 22 °C; 2: 25 °C; 3: 28 °C; 4: 30 °C; 5: 33 °C; 6: 37 °C.

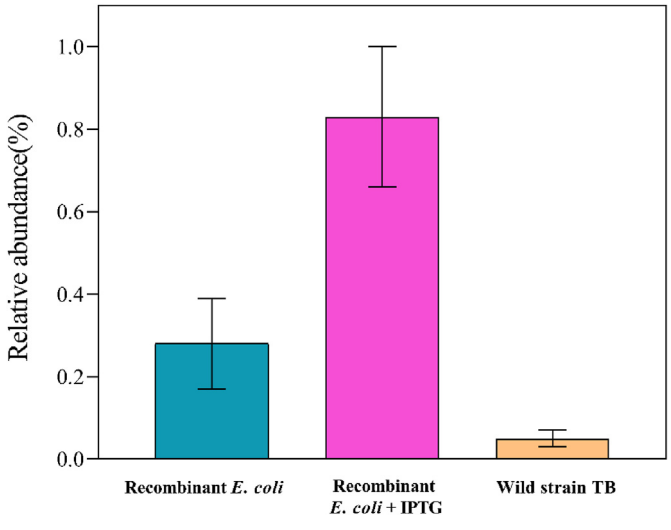

Fig. 5. The *norB* gene relative expression abundance in wild strain TB and recombinant *E. coli*.

genes. These results indicated that the denitrification mechanisms between *Achromobacter* and *Pseudomonas* were different, and the denitrifying bacteria of the same genus but different species may share similar denitrification mechanisms.

The recombinant *E. coli* BL21 (DE3) induced by IPTG showed an apparent band near 45 kDa; however, uninduced *E. coli* BL21 (DE3) and negative controls also showed bands at the same site. Thus, we examined the effect of different IPTG concentrations on *norB* gene expression. The yield of NorB protein varied with the concentration of IPTG, and the optimal concentration of IPTG was 1.0 mM, indicating that the *norB* gene was successfully expressed in recombinant *E. coli* BL21 (DE3). The yield of NorB was inhibited when IPTG concentrations were higher than 1.0 mM. Similarly, Einsfeldt et al. (2011) found that higher IPTG concentrations had a negative effect on cell growth and plasmid stability. The observed difference in relative expression abundance under IPTG induction was consistent with that in previous studies, which suggested that the level of gene transcription can be enhanced by using a suitable concentration of IPTG (Choi and Geletu, 2018). There was a phenomenon of background expression in recombinant *E. coli* without IPTG induction (Fig. 5). This may be because tryptone in the LB medium contains a trace amount of lactose or recombinant *E. coli* produces a lactose analog, thereby initiating the background expression of the *norB* gene (Chen et al., 2013).

To obtain better expression of the *norB* gene, the induction time

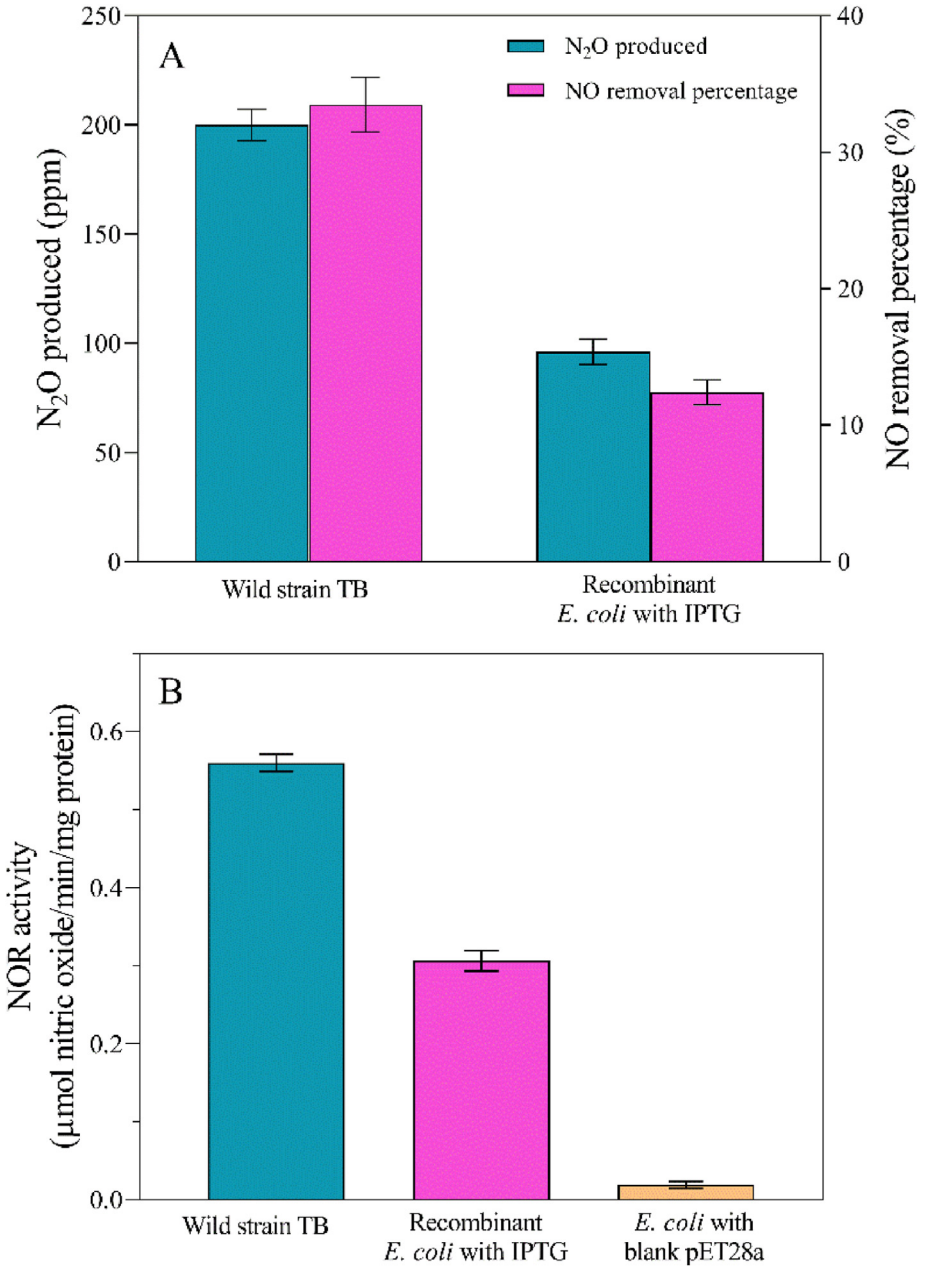

Fig. 6. Comparison of NO reduction performance (A) and NOR activity (B) in three strains.

and induction temperature that affect gene expression were optimized to 5 h and 30 °C, respectively. Because the bacterial cells are in the growth phase, the amount of bacterial cells continues to increase with the extension of the induction time. The enzyme production increased with the induction time but reached the maximum at 5 h. After bacteria grow to a stable period, prolonging the induction time further may cause problems such as hydrolysis and denaturation of the recombinant protein (Choi and Geletu, 2018; Vasconcelos et al., 2018). Almost no difference was observed in the results of the induced temperature. This may be because the overall expression level of NorB was relatively high after the optimal IPTG final concentration and induction time were determined. Thus, the difference in the effect of temperature on *norB* expression could not be easily distinguished from the SDS-PAGE gel image. In addition, recombinant *E. coli* itself can produce an endogenous protein of 45 kDa, which exacerbates the difficulty of differentiation. The reason why the optimal induction temperature was lower than the optimal growth temperature of recombinant *E. coli* was that the lower culture temperature can reduce proteolytic activity, resulting in higher yields (Badillo-Zeferino et al., 2017).

Recombinant *E. coli* can reduce NO to N_2O accompanied by the production of 96.27 ppm N_2O. The NO reduction efficiency of strain TB (33.48%) was 4.68 times higher than that of recombinant *E. coli*. However, the RT-qPCR results showed that the relative expression abundance of *norB* in strain TB was as low as 0.05%, and the total protein of strain TB had no target band of 45 kDa on the SDS-PAGE gel (Fig. 4). Therefore, the cloned *norB* gene in the recombinant *E. coli* was probably incomplete. The true NOR-encoding gene may also have some assistant sequence fragments that were transcribed together with gene *norB*. These assistant sequence fragments were important for increasing the enzymatic activity of NOR. Moreover,

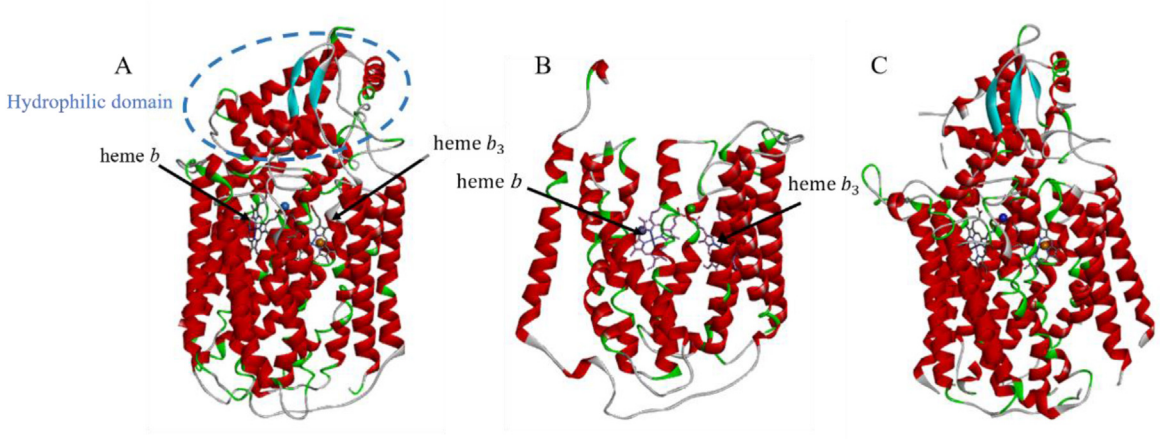

Fig. 7. Comparison of three protein spatial structures. (A) Predictive dimensional structure of NOR from strain TB (2286 bp); (B) Predictive dimensional structure of NorB (1218 bp); (C) Overall structure of qNOR from *N. meningitides*. The marked structural differences were highlighted by dotted circles.

previous studies have demonstrated that NOR has five conserved Glu residues, all of which are known to be functionally important in the catalytic NO reduction reaction (Shiro, 2012). The specific activity of recombinant wild-type cNOR obtained from the *P. aeruginosa* expression system was from 0.60 ± 0.30 to 30.00 ± 10.00 μmol-NO/s/μmol-cNOR (Yamagiwa et al., 2018). Owing to the lack of some important residues, the NOR activity was greatly affected. Gonska et al. (2018) found that variants retained NO reduction activity (40–100% of that of wild-type). Variant E259Q showed the best degradation ability with NO consumption rate (% wild-type) of 102 ± 5. While the NO consumption rate of variant E498f was only 1.5 ± 0.4, which is lower than the degradation efficiency of our recombinant *E. coli*.

On the basis of the above results, we recalibrated and reassembled the whole genome sequence of strain TB and obtained a 2286 bp-long NOR coding sequence, which is consistent with the NOR coding gene in *A. xylosoxidans* NCTC10807. This coding sequence contained not only the cloned *norB* (1218 bp) but also some other auxiliary fragments. The 2286 bp gene sequence was translated into 761 amino acids, and the molecular mass of the protein was calculated to be 84.2 kDa, which is basically consistent with that of the NOR encoded by the single gene *norB* in *R. eutropha* (Cramm et al., 1999). The NOR protein structure of TB encoded by 2286 bp *nor* gene was very similar to the overall structure of qNOR in *N. meningitides* (Fig. 7C), and both consisted of the catalytic reduction structure responsible for NO reduction (underside) and the auxiliary structure responsible for electron transfer (upside). Therefore, the 2286 bp-long gene sequence may be the full sequence encoding NOR in strain TB.

Cloned NorB protein appeared to be derived from the catalytic reduction structure of NOR in strain TB, and the amino acid sequence similarity was 75.96%, indicating that NorB protein is an important component of the NOR catalytic reduction structure in strain TB. Notably, although the crystal structures of cNOR and qNOR have been extensively studied, NOR encoded by a single gene *norB* has not yet received considerable attention. Comparing the NorB protein with the NOR protein structure of strain TB (Fig. 7A and B), two transmembrane helices from the C-terminal of NorB protein were apparently deleted. In addition, NorC-like structures were absent at the N-terminus of NorB protein. The overall structure of NorB was similar to the catalytic reduction structure composed of numerous transmembrane helices at the C-terminal of strain TB NOR. In this structure domain, heme b_3 and non-heme FeB constituted binuclear centers, which could bind to the NO and reduce it to N_2O and were similar to cNOR and cbb_3 oxidase (Buschmann et al., 2010; Gonska et al., 2018). In short, the core component of the NOR catalytic reduction structure can independently exert the NO reduction function. This result is in accordance with the study on the function of the LsrB protein substrate binding domain (Tang et al., 2017). Similarly, Sakurai et al. (2017) reported that the soluble domain of NOR without its anchor helix (NorC*), which functions as an electron acceptor from the intrinsic cytochrome *c*, was expressed in *E. coli*. The reason why the NO reduction performance of recombinant *E. coli* was considerably lower than that of strain TB is probably because the NorB protein lacks the auxiliary structure above responsible for promoting NOR enzyme activity based on the difference in the structure of the two proteins (Fig. 7A and B). These findings open an avenue for further research on the NOR structure and its function and broaden insights into the construction of recombinant bacteria.

5. Conclusions

The present study reported the genomic characteristics of the *A. denitrificans* strain TB. The results demonstrated that the *nar*, *nap*, *nirK*, *norB*, and *nos* genes were found to be involved in the pathway of denitrification, and the *norB* gene encoding a NOR catalytic reduction core peptide was obtained. Subsequently, the heterologous prokaryotic expression system of the *norB* gene was successfully constructed in *E. coli* BL21 (DE3). The relative expression abundance of the *norB* gene in the recombinant *E. coli* was increased by 16.6 times compared with that in the wild strain TB, and the NO reduction efficiency of the recombinant *E. coli* was 12.39% within 13 h. The three-dimensional structure of the NorB protein was predicted. These results indicate that the core peptide of the NOR catalytic reduction structure can independently exert NO reduction, and the lower NO reduction efficiency of the recombinant *E. coli* may be due to the loss of the auxiliary structure, which can enhance the NOR enzyme activity and plays an electronic transfer function.

Declaration of competing interest

The authors declare that they have no known competing financial interests or personal relationships that could have appeared to influence the work reported in this paper.

CRediT authorship contribution statement

Cong Chen: Formal analysis, Investigation, Writing - original

draft, Writing - review & editing. **Yu Wang:** Formal analysis, Investigation, Writing - original draft. **Huan Liu:** Validation, Data curation. **Yi Chen:** Validation, Formal analysis. **Jiachao Yao:** Writing - review & editing. **Jun Chen:** Methodology, Conceptualization, Resources, Writing - review & editing, Supervision. **Dzmitry Hrynsphanb:** Methodology, Validation. **Savitskaya Tatsianab:** Methodology.

Acknowledgments

The project was supported by the Natural Science Foundation of China (21777142), the National Primary Research & Development Plan(2018YFE0120300) and the Natural Science Foundation of Zhejiang Province (LY17E080018).

Appendix A. Supplementary data

Supplementary data to this article can be found online at https://doi.org/10.1016/j.chemosphere.2020.126739.

References

Abalos, D., Sanz-Cobena, A., Misselbrook, T., Vallejo, A., 2012. Effectiveness of urease inhibition on the abatement of ammonia, nitrous oxide and nitric oxide emissions in a non-irrigated Mediterranean barley field. Chemosphere 89, 310–318.

Badillo-Zeferino, G.L., Ruiz-Lopez II, Oliart-Ros, R., Sanchez-Otero, M.G., 2017. Improved expression and immobilization of Geobacillus thermoleovorans CCR11 thermostable recombinant lipase. Biotechnol. Appl. Biochem. 64, 62–69.

Buschmann, S., Warkentin, E., Xie, H., Langer, J.D., Ermler, U., Michel, H., 2010. The structure of cbb3 cytochrome oxidase provides insights into proton pumping. Science 329, 327–330.

Butland, G., Spiro, S., Watmough, N.J., Richardson, D.J., 2001. Two conserved glutamates in the bacterial nitric oxide reductase are essential for activity but not assembly of the enzyme. J. Bacteriol. 183, 189–199.

Chen, J., Gu, S., Hao, H., Chen, J., 2016. Characteristics and metabolic pathway of *Alcaligenes* sp. TB for simultaneous heterotrophic nitrification-aerobic denitrification. Appl. Microbiol. Biotechnol. 100, 9787–9794.

Chen, W.-B., Nie, Y., Xu, Y., Xiao, R., 2013. Enhancement of extracellular pullulanase production from recombinant *Escherichia coli* by combined strategy involving auto-induction and temperature control. Bioproc. Biosyst. Eng. 37, 601–608.

Chen, Y., Wang, Q., Zhao, S., Yang, W., Wang, H., Jia, W., 2019. Removal of nutrients and emission of nitrous oxide during simultaneous nitrification, denitrification and phosphorus removal process with metal ions addition. Int. Biodeterior. Biodegrad. 142, 143–150.

Choi, T.J., Geletu, T.T., 2018. High level expression and purification of recombinant flounder growth hormone in *E. coli*. J Genet Eng Biotechnol 16, 347–355.

Cramm, R., Pohlmann, A., Friedrich, B., 1999. Purification and characterization of the single-component nitric oxide reductase from *Ralstonia eutropha* H16. FEBS Lett. 460, 6–10.

Einsfeldt, K., Severo Júnior, J.B., Corrêa Argondizzo, A.P., Medeiros, M.A., Alves, T.L.M., Almeida, R.V., Larentis, A.L., 2011. Cloning and expression of protease ClpP from Streptococcus pneumoniae in *Escherichia coli*: study of the influence of kanamycin and IPTG concentration on cell growth, recombinant protein production and plasmid stability. Vaccine 29, 7136–7143.

Gomes, F.O., Maia, L.B., Loureiro, J.A., Pereira, M.C., Delerue-Matos, C., Moura, I., Moura, J.J.G., Morais, S., 2019. Biosensor for direct bioelectrocatalysis detection of nitric oxide using nitric oxide reductase incorporated in carboxylated single-walled carbon nanotubes/lipidic 3 bilayer nanocomposite. Bioelectrochemistry 127, 76–86.

Gonska, N., Young, D., Yuki, R., Okamoto, T., Hisano, T., Antonyuk, S., Hasnain, S.S., Muramoto, K., Shiro, Y., Tosha, T., Adelroth, P., 2018. Characterization of the quinol-dependent nitric oxide reductase from the pathogen *Neisseria meningitidis*, an electrogenic enzyme. Sci. Rep. 8, 3637.

Hino, T., Matsumoto, Y., Nagano, S., Sugimoto, H., Fukumori, Y., Murata, T., Iwata, S., Shiro, Y., 2010. Structural basis of biological N_2O generation by bacterial nitric oxide reductase. Science 330, 1666–1670.

Hong, Z., Wang, Z., Li, X.B., 2017. Catalytic oxidation of nitric oxide (NO) over different catalysts: an overview. Catal. Sci. Technol. 7, 3440–3452.

Kahle, M., ter Beek, J., Hosler, J.P., Ädelroth, P., 2018. The insertion of the non-heme FeB cofactor into nitric oxide reductase from *P. denitrificans* depends on NorQ and NorD accessory proteins. Biochim. Biophys. Acta Bioenerg. 1859, 1051–1058.

Kennes, C., Rene, E.R., Veiga, M.C., 2009. Bioprocesses for air pollution control. J. Chem. Technol. Biotechnol. 84, 1419–1436.

Li, C., Yang, J., Wang, X., Wang, E., Li, B., He, R., Yuan, H., 2015. Removal of nitrogen by heterotrophic nitrification-aerobic denitrification of a phosphate accumulating bacterium Pseudomonas stutzeri YG-24. Bioresour. Technol. 182, 18–25.

Matsumoto, Y., Tosha, T., Pisliakov, A.V., Hino, T., Sugimoto, H., Nagano, S., Sugita, Y., Shiro, Y., 2012. Crystal structure of quinol-dependent nitric oxide reductase from *Geobacillus stearothermophilus*. Nat. Struct. Mol. Biol. 19, 238–245.

Mazza, R., Mazzette, R., 2014. Absolute and Relative Gene Expression in Listeria Monocytogenes Using Real-Time PCR. Listeria monocytogenes, pp. 213–221.

Nadeau, S.A., Roco, C.A., Debenport, S.J., Anderson, T.R., Hofmeister, K.L., Walter, M.T., Shapleigh, J.P., 2019. Metagenomic analysis reveals distinct patterns of denitrification gene abundance across soil moisture, nitrate gradients. Environ. Microbiol. 21, 1255–1266.

Nasr, R., Akbari Eidgahi, M.R., 2014. Construction of a synthetically engineered *nirB* promoter for expression of recombinant protein in *Escherichia coli*. Jundishapur J. Microbiol. 7, 15942–15946.

Noi, N.V., Chung, Y.C., 2017. Optimization of expression and purification of recombinant S1 domain of the porcine epidemic diarrhea virus spike (PEDV-S1) protein in *Escherichia coli*. Biotechnol. Biotechnol. Equip. 31, 619–629.

Ramos, S., Almeida, R.M., Cordas, C.M., Moura, J.J.G., Pauleta, S.R., Moura, I., 2017. Insights into the recognition and electron transfer steps in nitric oxide reductase from *Marinobacter hydrocarbonoclasticus*. J. Inorg. Biochem. 177, 402–411.

Sakurai, N., Kataoka, K., Sugaya, N., Shimodaira, T., Iwamoto, M., Shoda, M., Horiuchi, H., Kiyono, M., Ohta, Y., Triwiyono, B., Seo, D., Sakurai, T., 2017. Heterologous expression of *Halomonas halodenitrificans* nitric oxide reductase and its N-terminally truncated NorC subunit in *Escherichia coli*. J. Inorg. Biochem. 169, 61–67.

Shiro, Y., 2012. Structure and function of bacterial nitric oxide reductases: nitric oxide reductase, anaerobic enzymes. Biochim. Biophys. Acta 1817, 1907–1913.

Sofya, K., Knaff, D.B., Masakazu, H., Bernard, L., Pierre, S., 2005. Mechanism of spinach chloroplast ferredoxin-dependent nitrite reductase: spectroscopic evidence for intermediate states. Biochemistry 43, 510–517.

Tang, G., Xing, S., Wang, S., Yu, L., Li, X., Staehelin, C., Yang, M., Luo, L., 2017. Regulation of cysteine residues in LsrB proteins from *Sinorhizobium meliloti* under free-living and symbiotic oxidative stress. Environ. Microbiol. 19, 5130–5145.

Tomasek, A., Staley, C., Wang, P., Kaiser, T., Lurndahl, N., Kozarek, J.L., Hondzo, M., Sadowsky, M.J., 2017. Increased denitrification rates associated with shifts in prokaryotic community composition caused by varying hydrologic connectivity. Front. Microbiol. 8, 2304.

Tosha, T., Shiro, Y., 2013. Crystal structures of nitric oxide reductases provide key insights into functional conversion of respiratory enzymes. IUBMB Life 65, 217–226.

Vasconcelos, L., Oliveira Filho, M.A., Ribeiro, V.T., Araujo, J.S., de Sousa Junior, F.C., Martins, D.R.A., Dos Santos, E.S., 2018. Optimization of the 503 antigen induction strategy of *Leishmania infantum chagasi* expressed in *Escherichia coli* M15. Prep. Biochem. Biotechnol. 48, 968–976.

Vedler, E., Vahter, M., Heinaru, A., 2004. The completely sequenced plasmid pEST 4011 contains a novel IncP1 backbone and a catabolic transposon harboring tfd genes for 2,4-dichlorophenoxyacetic acid degradation. J. Bacteriol. 186, 7161–7174.

Vincenzo, D.P., Simona, P., Gian Maria, R., 2014. Characterization of plasmid pAX 22, encoding VIM-1 metallo-β-lactamase, reveals a new putative mechanism of In70 integron mobilization. J. Antimicrob. Chemother. 69, 67–71.

Wang, H., Gunsalus, R.P., 2000. The *nrfA and nirB* nitrite reductase operons in *Escherichia coli* are expressed differently in response to nitrate than to nitrite. J. Bacteriol. 182, 5813–5822.

Wang, Y., Wang, Z., Duo, Y., Wang, X., Chen, J., Chen, J., 2018. Gene cloning, expression, and reducing property enhancement of nitrous oxide reductase from *Alcaligenes denitrificans* strain TB. Environ. Pollut. 239, 43–52.

Wasser, I.M., de Vries, S., Moenne-Loccoz, P., Schroder, I., Karlin, K.D., 2002. Nitric oxide in biological denitrification: Fe/Cu metalloenzyme and metal complex NOx redox chemistry. Chem. Rev. 102, 1201–1234.

Yamagiwa, R., Kurahashi, T., Takeda, M., Adachi, M., Nakamura, H., Arai, H., Shiro, Y., Sawai, H., Tosha, T., 2018. *Pseudomonas aeruginosa* overexpression system of nitric oxide reductase for in vivo and in vitro mutational analyses. Biochim. Biophys. Acta Bioenerg. 1859, 333–341.

Yan, Y., Jian, Y., Dou, Y., Ming, C., Ping, S., Peng, J., Wei, L., Wei, Z., Yao, Z., Li, H., 2008. Nitrogen fixation island and rhizosphere competence traits in the genome of root-associated *Pseudomonas stutzeri* A1501. Proc. Natl. Acad. Sci. U. S. A 105, 7564–7569.

Yoon, S., Nissen, S., Park, D., Sanford, R.A., Loffler, F.E., 2016. Nitrous oxide reduction Kinetics distinguish bacteria harboring clade I NosZ from those harboring clade II NosZ. Appl. Environ. Microbiol. 82, 3793–3800.

Zhao, B., Cheng, D.Y., Tan, P., An, Q., Guo, J.S., 2018. Characterization of an aerobic denitrifier *Pseudomonas stutzeri* strain XL-2 to achieve efficient nitrate removal. Bioresour. Technol. 250, 564–573.

Zumft, W.G., 2005. Nitric oxide reductases of prokaryotes with emphasis on the respiratory, heme-copper oxidase type. J. Inorg. Biochem. 99, 194–215.